A revised spray-combustion diagram of diffusion-controlled burning regimes in fuel-spray clouds

By J. Urzay

1. Motivation and objectives

Fuel droplets in combustors interact strongly with flames and turbulence in practical liquid-fueled combustors of terrestrial and aerial propulsion systems (Williams 1965; Sirignano 1999). Although a great deal of physical understanding has been achieved in purely gaseous combustion over the last century, not much is currently known about spray combustion at the fundamental level. In this short note, a revision of earlier combustion-regime diagrams for non-premixed spray combustion of stationary fuel clouds (Chiu, Kim & Croke 1982) is done that includes fuel-oxidizer stoichiometry characteristics and the radius of a single-droplet flame. By doing so, this study suggests that the the group-combustion number may not be the sole indicator of each spray-combustion mode. The resulting diagram describes the burning regimes in the fuel-spray cloud by making use of two dimensionless parameters, namely, the mass-loading ratio and the vaporization Stokes number, which appear naturally in the nondimensional form of the conservation equations.

2. A revised non-premixed spray-combustion-regime diagram for diffusion-controlled fuel-spray clouds

Traditional descriptions of spray combustion in non-premixed systems follow earlier work by Chiu *et al.* (1982), in which a quasi-stationary monodisperse cloud of radius a_c carries a uniform distribution of n droplets per unit volume, each droplet having a radius a and density ρ_d. An oxidizing gas, which has a density ρ and thermal diffusivity D_T, surrounds the fuel cloud at rest. In the fast-chemistry limit, the chemical time is the shortest of all time scales, and combustion is controlled solely by diffusion. In this limit, the characteristic time scales describing the vaporization and combustion processes in the fuel cloud are the diffusive time $t_c = a_c^2/D_T$ of heat into the cloud, the vaporization time $t_v = (\rho_d/\rho)(a^2/D_T)$ of each droplet, and the characteristic time scale of variation of the mass and thermal energy in the ambient gas produced by the vaporization process $t_g = (4\pi D_T a n/3)^{-1}$. The vaporization time t_v is obtained from a balance between the heat transferred from the gas to the droplet and the thermal energy used for vaporization, with the additional assumption that $c_p(T - T_B)/L_v$ is an order-unity parameter, where T is the local hot temperature driving vaporization, L_v is the latent heat of vaporization, and T_B is the boiling temperature of the fuel. The spray-gas interaction time scale t_g is obtained from a balance between the convective terms in the continuity or energy equations of the gas and the corresponding spray-source terms. Additionally, in this analysis, unity Lewis numbers are assumed for both fuel and oxidizer.

Earlier work (Chiu *et al.* 1982) proposed that the nondimensional group-combustion

number,

$$\mathrm{G} = \frac{t_c}{t_g} = \frac{4\pi a_c^2 a n}{3} = \left(\frac{a_c}{a_g}\right)^2, \tag{2.1}$$

is the main parameter for describing the fast-combustion regimes found in this problem. In eq. (2.1), $a_g \sim (4\pi n a/3)^{-1/2}$ is a characteristic thermal penetration length in the spray cloud, obtained from balancing the heat diffusion and vaporization terms in the gas energy equation. In this way, large values of G imply long diffusion times in the spray cloud and large amounts of energy from the gas needed for vaporization, thereby restraining combustion and vaporization to occur only in thin superficial layers of thickness of $O(\mathrm{G}^{-1/2})$ with respect to the cloud radius a_c, as indicated by a diffusion-vaporization balance. Small values of G represent short diffusion times and rapid heating of the cloud without much distortion of the surrounding gas, thereby enhancing distributed droplet combustion and vaporization in internal regions of the cloud. Since the number of droplets in the cloud is $N = 4\pi a_c^3 n/3$ and the droplet interspace distance is $\delta_d = (4\pi n/3)^{-1/3}$, the parameter G represents a relation between the number of droplets N and the dimensionless droplet interspacing δ_d, namely $\mathrm{G} \sim N^{2/3} a/\delta_d$.

Based on eq. (2.1), Chiu *et al.* (1982) described a combustion-regime diagram in a $\{(\delta_d/a),\, N\}$ coordinate system, in which delimitations in the combustion characteristics are traced by using solely G =constant lines in the following manner. For $\mathrm{G} \gg 1$ an external sheath-combustion regime occurs, in which there is not sufficient time for the heat to diffuse in the cloud and produce droplet vaporization. In this regime, vaporization occurs on the cloud surface in a thin layer of thickness of $O(\mathrm{G}^{-1/2})$ with respect to the cloud radius, in which heat diffusion balances vaporization energy. In this limit, the temperature of the liquid phase decays rapidly in spatial scales of $O(\mathrm{G}^{-1/2})$ from the boiling temperature T_B at the cloud boundary to the initial temperature of the liquid droplets in the cloud. Provided that the Damköhler number is sufficiently large, the fuel vaporized in the outer shell of the cloud burns in a diffusion flame that envelops the cloud. This regime is encountered only in large and dense spray clouds, $a_c/\delta_d \gg (\delta_d/a)^{1/2}$. As G decreases toward order-unity values by, for instance, decreasing the droplet-number density n or the cloud radius a_c, the vaporization zone penetrates in the central region of the cloud. For $\mathrm{G} = O(1)$ an external group-combustion regime exists, in which the time needed for heat diffusion in the cloud is sufficiently long to vaporize the droplets inside; in this regime, the liquid in the central region of the cloud is at the boiling temperature and, similar to the large-G case, the fuel vapor burns in a diffusion flame that envelops the cloud. For $\mathrm{G} \lesssim O(1)$ an internal group-combustion regime takes place as an intermediate limit between external sheath-combustion and single-droplet combustion; in this regime, the droplets vaporize without combustion in the central region of the cloud, which is surrounded by a diffusion flame and by an outer region of a similar size in which individual droplet burning occurs. Finally, for $\mathrm{G} \ll 1$, the heat-diffusion time in the cloud is much shorter than the spray-gas interaction time, and each droplet burns individually with a surrounding flame.

In this study, the description given Chiu *et al.* (1982) -namely the single-parameter description of the regimes in terms of G described above- is revised for including the flame radius of a burning droplet as additional length and a measure of air-fuel stoichiometry characteristics. In particular, the single-droplet combustion regime cannot occur unless the droplet interspacing δ_d is larger than the flame diameter, which is denoted here as $2a_f$. It is therefore more expedient to include a second parameter in the description of the combustion regimes that relates the droplet radius to the droplet interspacing

independently of the number of droplets within the cloud or its dimensions. The sought parameter is the mass of liquid per unit mass of gas in the spray,

$$\alpha = \frac{t_v}{t_g} = \frac{(4/3)\pi\rho_d a^3 n}{\rho} = \left(\frac{\rho_d}{\rho}\right)\left(\frac{a}{\delta_d}\right)^3, \tag{2.2}$$

which corresponds to a mass-loading ratio in engineering terminology. As α increases, the spray dilution decreases, and the enveloping flame expands in search of equilibrium positions in which the value of the fuel-vapor mass fraction has decayed sufficiently for the fuel to burn with oxygen in stoichiometric proportions. The critical value of α for which the droplet interspacing equals the flame diameter, $\delta_d = 2a_f$, is denoted here as α_f. The flame radius around an individual droplet a_f can be calculated by using large-activation-energy analyses for unity Lewis numbers (Williams 1965), which gives

$$\alpha_f = \left(\frac{\rho_d}{8\rho}\right)\left\{\frac{\ln\left(\dfrac{1+S_L}{S_L}\right)}{\ln\left[1+\dfrac{c_p(T-T_B)+q/S_L}{L_v}\right]}\right\}^3, \tag{2.3}$$

with q the chemical heat released. In the formulation, $S_L = s/Y_{\mathrm{O}_2}$ is a local stoichiometric coefficient in which s is the mass of oxidizer burnt per unit mass of fuel in stoichiometric conditions and Y_{O_2} is the local oxidizer mass fraction in the surroundings of the fuel droplet. Note that eq. (2.3) is accurate only for sufficiently small Péclet numbers $\mathrm{Pe}_d = |\mathbf{v}-\mathbf{v}_d|a/D_T \ll 1/S_L \ll 1$, for which the flame sits within the Stokes region where relative advection is not important, with $\mathbf{v}$ and $\mathbf{v_d}$ being, respectively, the gas and droplet velocity vectors. Since S_L is typically large in hydrocarbon-air combustion, the approximation $a/a_f \sim 1/S_L$ is made, and the mass-loading ratio for which the droplet interspace becomes equal to the flame diameter is $\alpha_f \sim \rho_d/(8\rho S_L^3)$, which ranges from 0.001 for $\rho_d/\rho \sim 10^3$ and $S_L \sim 10$, to 0.1 for $\rho_d/\rho \sim 10^2$ and $S_L \sim 15$. In considering highly loaded sprays, a rather non-conservative upper limit $\alpha \sim \rho_d/\rho$ may be identified beyond which the droplet interspacing becomes of the same order as the droplet radius, $a/\delta_d \sim 1$; in this large-loading limit, which is equivalent to order-unity liquid-volume fractions, every attempt to address spray vaporization or combustion is inadequate if Lagrangian or Eulerian formulations are used with source terms calculated from single-droplet dynamics. However, a much smaller maximum threshold of the mass-loading ratio is required for the consistency of of both micro and mesoscale modelling of spray flows, in that typical microscale formulations for calculating source terms need integration-domain sizes of order $(\rho_d/\rho)^{1/2}a$ or larger for the quasi-steady convective-diffusive vaporization formulation to be accurate, especially if low-Péclet number approximations are used, thereby yielding a minimum allowable droplet separation distance of order $a/\delta_d \sim (\rho/\rho_d)^{1/2}$ and a maximum mass-loading ratio $\alpha \sim (\rho/\rho_d)^{1/2}$, which are equivalent to liquid-volume fractions of $O(\rho/\rho_d)$.

For the extended description proposed in this study, an additional parameter is needed, namely, the vaporization Stokes number

$$\mathrm{St}_v = \frac{t_v}{t_c} = \frac{\alpha}{\mathrm{G}} = \left(\frac{\rho_d}{\rho}\right)\left(\frac{a}{a_c}\right)^2, \tag{2.4}$$

which represents the ratio of the single-droplet vaporization time t_v to the diffusion time of heat into the cloud t_c. That the vaporization Stokes number is an essential parameter in any description of spray combustion can be observed by noticing that the source

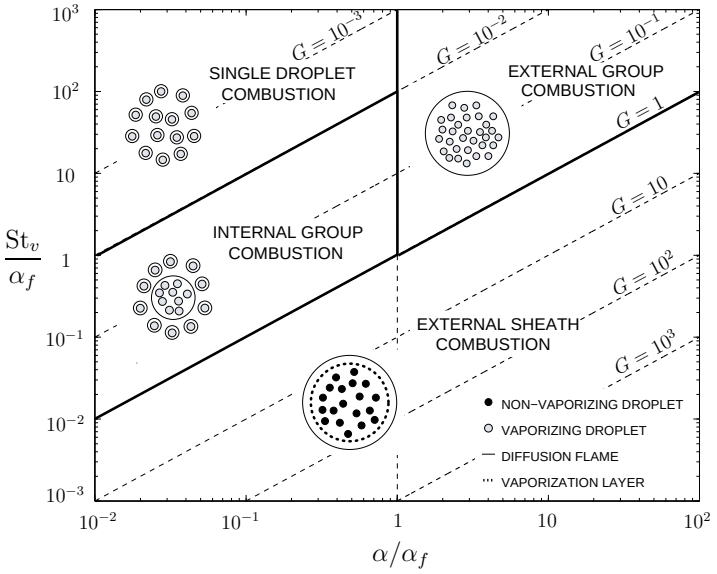

FIGURE 1. Revised Chiu's diagram for non-premixed combustion of fuel-spray clouds. The definitions of the nondimensional group-combustion number G, the mass-loading ratio α, and the vaporization Stokes number St_v are given, respectively, in equations (2.1), (2.2) and (2.4). The critical mass-loading ratio α_f is given in eq. (2.3).

terms in the liquid-phase conservation equations are premultiplied by a factor $1/\mathrm{St}_v$ after nondimensionalization is made with velocity and length scales from the gas phase. This is in contrast to the source terms in the gas-phase conservation equations, which represent the strength of the liquid-phase effects on the gas phase, and which become premultiplied by G when characteristic scales from the gas phase are used for nondimensionalization.

Based on the above considerations, it is more expedient to classify the spray-combustion regimes in a dimensionless $\{\alpha, \mathrm{St}_v\}$ diagram instead of the $\{(\delta_d/a), N\}$ diagram used earlier by Chiu *et al.* (1982), because, according to the formulation given above, different combustion regimes can develop for the same value of the group-combustion number G as a result of different values of the mass-loading ratio α. Therefore, even in this simplified scenario, the group-combustion number G cannot be the sole indicator of the occurrence of the different spray-combustion modes.

From this revision, the spray-combustion regime diagram shown in figure 1 is obtained. Note that the diagram $\{\alpha, \mathrm{St}_v\}$ is fuel dependent, since α_f depends on the fuel-air stoichiometry characteristics. However, this dependency can be ruled out by normalizing the diagram axes with α_f. For $\mathrm{G} \gg 1$, the external sheath combustion regime previously envisioned by Chiu *et al.* (1982) still occurs in this revised description. For $\mathrm{G} = O(1)$ the vaporization layer thickness has grown inward to a distance comparable to the radius of the cloud, and a transition occurs from external sheath-combustion to either external group-combustion or internal group-combustion regimes, depending on the liquid mass loading α. In particular, external group-combustion occurs for $\mathrm{G} = O(1)$ and $\alpha/\alpha_f > 1$, or equivalently, for $\delta_d < 2a_f$. In this regime, all droplets in the cloud undergo vaporization, and since the droplet interspacing is smaller than the flame radius of a single droplet, a single diffusion flame envelops the cloud. Internal group-combustion occurs for $\mathrm{G} = O(1)$ and $\alpha/\alpha_f < 1$, or, equivalently, for $\delta_d > 2a_f$. This is an intermediate and transient regime toward incipient single-droplet combustion, in which all droplets in the cloud

undergo vaporization, but since the droplet interspacing is larger than the flame radius of a single droplet, diffusion flames surrounding each droplet on the outer region of the cloud can be found, and a diffusion flame, which envelops the spray core where external group-combustion is taking place, retreats towards the center of the cloud in search of the zone in which the mixture fraction attains the stoichiometric value. For $\mathrm{G} \ll 1$, the time needed for the ambient thermal energy to diffuse inside the cloud is much faster than the spray-gas interaction time and all droplets undergo vaporization. However, unless $\alpha/\alpha_f < 1$, or, equivalently, unless $\delta_d > 2a_f$, a diffusion flame around a single droplet cannot be sustained. Therefore, in the small-G limit, single-droplet combustion occurs for $\alpha/\alpha_f < 1$, and external group-combustion takes place for $\alpha/\alpha_f > 1$.

3. Conclusions

In this short note, a revision of earlier work on spray-combustion regimes for diffusion-controlled fuel-droplet clouds is proposed that includes the fuel-air stoichiometry characteristics and the radius of a single-droplet flame. The simplistic reasoning above suggests that the the group-combustion number may not be the sole indicator of each spray-combustion mode since there is a critical mass-loading ratio above which single-droplet combustion is not expected to be sustainable.

Notwithstanding the unprecedented difficulties that are found when attempting to describe spray-combustion phenomena in swirl burners (Luo, Pitsch, Pai & Desjardins 2011), the reasoning given above in terms of G, α and St_v, may be helpful for understanding the physical processes involved in spray combustion in simplified problems. However, it should be emphasized that droplet-kinematic effects are not considered in the fuel-cloud problem since there is no flow time scale, and therefore the kinematic Stokes number does not appear in the description. Earlier work has attempted to treat the effects of droplet kinematic inertia (Reveillon & Vervisch 2005), but it is challenging to envision universal diagrams if these effects are included, although they are very important in many practical applications. Similarly, the analysis outlined here is valid only at large Damköhler numbers in which the fuel vapor burns vigorously in thin diffusion flames after vaporization, which is a questionable assumption when the fuel droplets move relative to the gas and finite Péclet-number effects need to be taken into account.

The occurrence of different spray-combustion regimes can be observed experimentally in canonical scenarios such as premixed flames in tubes (Burgoyne & Cohen 1954) and counterflow diffusion flames (Li 1997). Predictions of pollutant emissions from spray-flame calculations are expected to be largely influenced by the microscale modelling of this wealth of spray-combustion phenomena.

REFERENCES

Burgoyne, J. H. & Cohen, L. 1954 The effect of drop size on flame propagation in liquid aerosols. *Proc. Roy. Soc.* **225** (1162), 375–392.

Chiu, H. H., Kim, Y. & Croke, J. 1982 Internal group combustion of liquid droplets. *Proc. Combust. Inst.* **19**, 971–980.

Li, S. C. 1997 Spray stagnation flames. *Prog. Energy Combust. Sci.* **23**, 303–347.

Luo, K., Pitsch, H., Pai, M. G. & Desjardins, O. 2011 Direct numerical simulations and analysis of three-dimensional n-heptane spray flames in a model swirl combustor. *Proc. Combust. Inst.* **33**, 2143–2152.

Reveillon, J. & Vervisch, L. 2005 Analysis of weakly turbulent dilute-spray flames and spray combustion regimes. *J. Fluid Mech.* **537**, 317–347.

Sirignano, W. A. 1999 *Fluid dynamics and transport of droplets and sprays.* Cambridge University Press.

Williams, F. A. 1965 *Combustion Theory.* Addison-Wesley.